JOURNAL OF AGRICULTURAL AND FOOD CHEMISTRY

Article

Cite This: J. Agric. Food Chem. 2019, 67, 1244−1253

pubs.acs.org/JAFC

Visualized Detection of *Vibrio parahaemolyticus* in Food Samples Using Dual-Functional Aptamers and Cut-Assisted Rolling Circle Amplification

Shixi Song,[†] Xingyu Wang,[*,†] Ke Xu,[‡] Guanmei Xia,[†] and Xingbin Yang[*,†]

[†]Shaanxi Engineering Laboratory for Food Green Processing and Safety Control, Shaanxi Key Laboratory for Hazard Factors Assessment in Processing and Storage of Agricultural Products, College of Food Engineering and Nutritional Science, Shaanxi Normal University, Xi'an, Shaanxi 710062, People's Republic of China

[‡]Department of Joint Surgery, Hong Hui Hospital, Xi'an Jiaotong University, Xi'an, Shaanxi 710054, People's Republic of China

Supporting Information

ABSTRACT: A biosensor using two aptamers (Dual-Apt) and cut-assisted rolling circle amplification (CA-RCA) for rapid and visualized detection of *Vibrio parahaemolyticus* was established. The anchoring aptamer (A-Apt) that specifically binds to the surface of *V. parahaemolyticus* was applied to separate and enrich the bacterium from the food matrix with the help of streptavidin magnetic beads. While the detecting aptamer (D-Apt), binding on the different sites of the cell surface, was used as a signal reporter. CA-RCA with an enhanced amplification rate was fabricated here to amplify the D-Apt to produce the monomeric G4 sequence that catalyzes the oxidation of $ABTS^{2-}$, resulting in the coloration visible to the naked eye. Under optimal conditions, as low as 10 colony-forming units (CFU)/mL (g) of *V. parahaemolyticus* can be visibly detected in real food samples. Free from DNA extraction, visualized signal output and no need for expensive instruments enable Dual-Apt and CA-RCA to be a promising strategy for on-spot rapid detection.

KEYWORDS: *aptamer, Vibrio parahaemolyticus, visualized detection, rolling circle amplification, G-quadruplex, magnetic separation*

INTRODUCTION

Food-borne disease, which poses a great threat to public health, has increased at an accelerating rate over the past few decades.[1] Among a multitude of prevailing pathogenic bacteria, such as *Salmonella*, *Escherichia coli*, *Listeria monocytogenes*, and *Staphylococcus aureus*, *Vibrio parahaemolyticus* is one of the most frequently reported food-borne pathogens.[2,3] According to the data in China's *Health and Family Planning Statistical Yearbook*, *V. parahaemolyticus* caused 72−147 disease cases between 2011 and 2015, leading annually to 1689 patients with symptoms of acute gastroenteritis, vomiting, fever, diarrhea, and abdominal cramps.[4] As a result of the strong halophilic nature of *V. parahaemolyticus*, seafoods, including shrimp, crab, squid, codfish, scallop, etc., tend to be contaminated by the bacterium, leading to huge economic losses.[5,6] Particularly, salted products (bacon, pickle, and salted duck egg), where growth of common pathogens barely occurred, could also be infected by *V. parahaemolyticus*. Individuals who take the raw or uncooked foods carrying that pathogen may result in food poisoning characterized by nausea, vomiting, diarrhea, fever, and even death in some serious cases. Therefore, developing robust methods for rapid and precise detection of *V. parahaemolyticus* is necessary for proper regulation of food safety and for entry−exit inspection and quarantine.

Traditionally, the plate counting method with specific medium for *V. parahaemolyticus* was applied to detect the pathogen. Although the method was reliable and accurate, its long process and laborious operation stand in the way of promoting it to the point-of-care detection. Therefore, several novel strategies, such as antibody-mediated immunological assay, polymerase chain reaction (PCR)-based methods, and isothermal amplification approaches [loop-mediated isothermal amplification (LAMP), strand displacement amplification (SDA), nucleic acid sequence-based amplification (NASBA), etc.], have been developed for *V. parahaemolyticus* diagnosis.[7−9] These strategies are proven to be of desirable specificity and sensitivity; however, requirement of expensive apparatuses and well-trained technicians hampered their widespread applications. For example, detectors for fluorescent signals have to be equipped to interpret the results for the LAMP- and NASBA-based strategies. Immunoassays could be applied for the detection of the viable pathogen, but the high cost and instability of antibodies, which play a key role for the pathogen recognition, are still limitations for those methods.[10] In some PCR-based detection strategies, false-positive results might be obtained for cross-contamination of samples.[11] The DNA extraction procedure added the complexity to the methods targeting nucleic acids of the pathogens. Besides, the presence of food ingredients, such as protein, polysaccharides, or lipids, could inhibit the detecting reaction, resulting in false-negative results.

Aptamers, obtained by systematic evolution of ligands by exponential enrichment (SELEX), are oligonucleotides capable of binding to different targets with high affinity comparable to that of the antibody.[12−14] On account of its high stability, low

Received: September 8, 2018
Revised: December 21, 2018
Accepted: January 3, 2019
Published: January 4, 2019

DOI: 10.1021/acs.jafc.8b04913
J. Agric. Food Chem. 2019, 67, 1244−1253

cost, and accessibility to chemical modifications, aptamers have become a powerful tool for highly sensitive detection, especially for bacteria in environmental and food samples, and have shown desirable feasibility and reliability.[15−17] The aptamer-based detections are rapid and robust and can be readily altered for detections with special requirements. In comparison to an antibody, the great advantage of an aptamer is that it can replicate itself, generating the amplified signals that greatly enhance the detection sensitivity.[18] Recently, advances have been made using aptamers to probe the presence of *V. parahaemolyticus*.[19−22] Those methods are proven to be of desirable specificity and sensitivity, demonstrating the potential of aptamers to construct efficient and reliable strategies for *V. parahaemolyticus* analysis in food samples.

In this study, we developed an aptamer-based sensing platform for visualized and rapid detection of *V. parahaemolyticus* in food samples. The *V. parahaemolyticus*-specific aptamers were selected from a random ssDNA library using a novel cell SELEX method (paper published elsewhere), and four aptamers with high affinity to *V. parahaemolyticus* cells were obtained. Two of the four aptamers, functionalized by directed chemical modification, were chosen. The anchoring aptamer (A-Apt) that was modified by biotin was used to capture and enrich *V. parahaemolyticus* cells with the help of streptavidin magnetic bead (SMB) separation. The detecting aptamer (D-Apt), covalently linked with a sequence that encodes a G-quadruplex structure (G4), was used as the template for cut-assisted rolling circle amplification (CA-RCA), where two types of nicking enzymes were employed to cut the nascent single strand to enhance the amplification rate up to 10^6 as well as to produce a monomeric G4 sequence. Visual detection can be realized by CA-RCA products containing the G4 structure that catalyzes the oxidation of $ABTS^{2-}$ with the help of hemin, resulting in a green color visible for the naked eye. Hence, a visualized biosensor, Dual-Apt and CA-RCA, which is capable of rapidly detecting less than 10 colony-forming units (CFU) of *V. parahaemolyticus* in food products, was established.

MATERIALS AND METHODS

Reagents. NaCl alkaline peptone water (3%), thiosulfate−citrate−bile salts−sucrose (TCBS), and Tween 20 were purchased from Solarbio Science & Technology Co., Ltd. (Beijing, China). Phosphate-buffered saline (PBS) solution was provided by HyClone (Logan, UT, U.S.A.). Φ29 DNA polymerase, T4 DNA ligase, and PEG 4000 were purchased from Thermo Scientific (Pittsburgh, PA, U.S.A.). SMB, Nb.BbvCI, and Nb.Btsl were purchased from New England Biolabs (Ipswich, MA, U.S.A.). SYBR Green I was provided by Life Technologies (Carlsbad, CA, U.S.A.). Bovine serum albumin (BSA) and proteinase K were obtained from Takara Bio, Inc. (Shanghai, China). *V. parahaemolyticus* (ATCC 17802), *E. coli* (ATCC 25922), *L. monocytogenes* (ATCC 19115), *Salmonella typhimurium* (ATCC 50761), *Shigella dysenteriae* (ATCC 13313), and *S. aureus* (ATCC 6538) were provided by the American Type Culture Collection (ATCC). All of the oligonucleotides used in the present study were synthesized and purified with high-performance liquid chromatography (HPLC) by Sangon (Shanghai, China) and used without further purification. The solutions used in this study were prepared by Milli-Q purified water (resistance < 18.2 MΩ cm^{-1}).

Bacteria Culture. The 3% NaCl alkaline peptone water medium was used to culture *V. parahaemolyticus* at 37 °C for 18 h. Lysogeny broth (LB) medium was used to culture *E. coli* and *S. aureus* at 37 °C for 12 h. The other bacteria were grown on BBL broth at 37 °C overnight. All of the liquid cultures were shaken at the speed of 120 revolutions/min.

For the CFU test of *V. parahaemolyticus*, the bacterium was cultured in 3% NaCl alkaline peptone water medium for 18 h. The cell suspension was subjected to gradient dilution. Then, 50 μL of each gradient was plated on TCBS dishes in triplicate, followed by incubation at 37 °C for 24 h, to allow the bacterium to grow. Then, colonies were counted, and the average numbers of three parallel dishes were recorded.

Enrichment of *V. parahaemolyticus*. Two aptamers, A-Apt and D-Apt, binding to different surface transmembrane proteins of *V. parahaemolyticus* cells, were employed. Bacteria suspensions varying in concentration were mixed with a certain amount of aptamers (A-Apt, 0.05 μM; D-Apt, 0.05 μM) in a final volume of 100 μL and incubated at 37 °C for 30 min. Then, SMBs of 10 μL were added, and the resulting solution was kept at room temperature for another 5 min with intermittent shaking. The SMB loading bacteria via A-Apt were then collected by magnet separation and transferred to a new Eppendorf tube, followed by washing twice using PBS containing 0.05% Tween and 4 μg/mL BSA. The SMB−aptamer−bacteria complexes were recollected and suspended by 20 μL of buffer solution for the following experiments.

Fabricating of CA-RCA for Visualized Detection of *V. parahaemolyticus*. CA-RCA was employed here to amplify the D-Apt containing the G4 decoding sequence, generating the visualized signal specifically indicating the presence of *V. parahaemolyticus*. The D-Apt was first circularized by T4 DNA ligase with the help of the Splint-L that was complementary to the two ends of the D-Apt. An aliquot of 5 μL solution containing D-Apt was added to 9.5 μL of reaction mixture, including 1× ligation buffer [40 mM Tris−HCl, 10 mM $MgCl_2$, 10 mM dithiothreitol (DTT), 5 mM adenosine triphosphate (ATP) at pH 7.8], 1 μL of 50% PEG 4000, and 1.0 μM Splint-L. The mixture was incubated at 95 °C for 5 min and slowly cooled to room temperature. Then, 0.5 μL of T4 DNA ligase (10 units/μL) was added, and the reaction was carried out at 25 °C for 10 min. CA-RCA was carried out by mixing the ligation product with 2.5 units of Φ29 DNA polymerase, a certain amount of nicking enzymes (Nb.BbvCI and Nb.Btsl), and 500 μM dNTPs in 1× Φ29 DNA polymerase buffer (33 mM Tris−Ac, 10 mM $MgAc_2$, 66 mM KAc, 10 mM DTT, and 1% Tween) with a total volume of 20 μL. The resulting mixture was incubated at 30 °C for 40 min. Then, aliquots of 10 μL of CA-RCA products were added to 10 μL of 2× 4-(2-hydroxyethyl)-1-piperazineethanesulfonic acid (HEPES) buffer containing 50 μM hemin, followed by incubating the mixture at 65 °C for 10 min to form the G4−hemin catalyzing complex. Then, the mixture of 20 μL was added to 250 μL of solution containing 6 mM $ABTS^{2-}$ and 60 mM H_2O_2, and the color developed by oxidation of $ABTS^{2-}$ to $ABTS^{\bullet -}$ could be observed. For high-throughput detection, 96-well plates were employed and the operation was the same as described before.

Detection of *V. parahaemolyticus* in Food Using Dual-Apt and CA-RCA. The sensitivity and specificity of detecting *V. parahaemolyticus* was evaluated using bacteria-spiked food products. Foods that are easily infested by *V. parahaemolyticus*, such as codfish, shrimp, milk, oysters, clams, squid, and jellyfish, were used as samples. The confirmed *V. parahaemolyticus*-negative foods (0.2 g/mL) were spiked with different amounts of *V. parahaemolyticus* cells to make sure that the final concentrations were in the range from 10^6 to 10 CFU/mL (g). The solid samples were cut into small pieces, followed by homogenization with a high-speed disperser (IKA, Staufen, Germany), in a final volume of 2 mL of PBS containing 0.05% Tween and 4 μg/mL BSA. The homogenate of 450 μL was added with a certain amount of A-Apt and D-Apt to make sure their final concentrations were 0.1 μM. The resulting mixture was placed under room temperature for 5 min, followed by the addition of 10 μL of SMBs under room temperature for another 5 min with intermittent shaking. The rest of the procedure was carried out as described in the above two experimental sections. For samples hard to homogenize, proteinase K treatment was applied. Briefly, 50 μL of proteinase K (10 mg/mL) was added to the spiked food sample, and the mixture was

DOI: 10.1021/acs.jafc.8b04913
J. Agric. Food Chem. 2019, 67, 1244−1253

Scheme 1. Schematic Illustration of Dual-Apt and CA-RCA for Visualized Detection of *V. parahaemolyticus* in Food

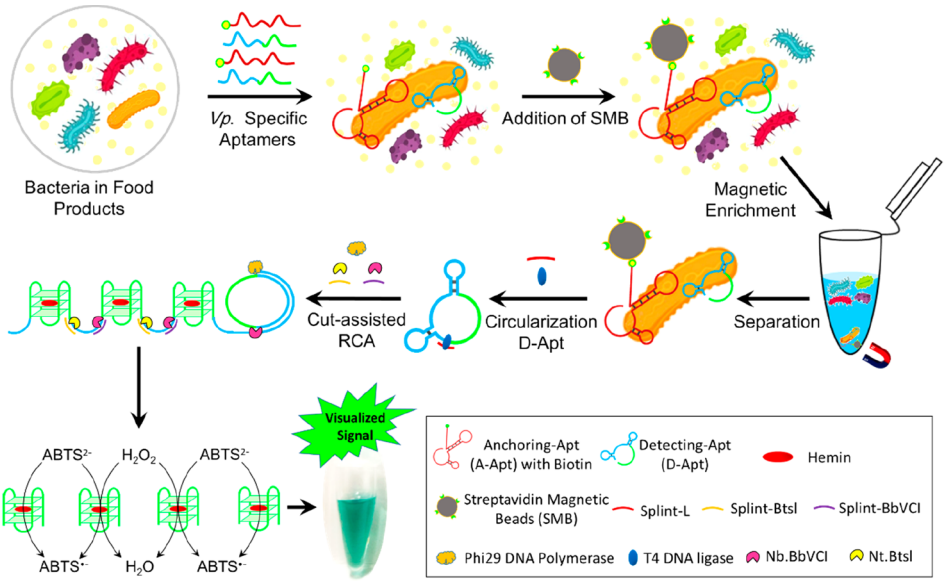

incubated at 37 °C for 30 min to digest the food protein. Then, proteinase K was inactivated by heat at 80 °C for 20 min for the following detection operation.

Comparison to Conventional Detection Methods. The contaminated food samples were also analyzed by the traditional methods of plate counting and PCR detection. The plate counting on specific medium was carried out according to the literature, with modification.[23] For PCR detection, a virulence gene, thermostable direct hemolysin (TDH) was used as the target, and the gene-specific primers were (5′ → 3′) forward, GTAAAGGTCTCTGACTTTTG-GAC, and reverse, TGGAATAGAACCTTCATCTTCACC.[24] Genomic DNA of *V. parahaemolyticus* was extracted using the fungal/bacterial DNA extract kit (Tiangen, Beijing, China). An aliquot of 5 μL of solution served as the template in a 20 μL amplification system containing 20 mM Tris−HCl (pH 8.8), 10 mM $(NH_4)_2SO_4$, 2.0 mM $MgSO_4$, 1.0 mg/mL BSA, 1.0% Triton X-100, 0.25 mM dNTPs, 0.2 μM of each primer, and 1.25 units of Pfu DNA polymerase. The PCR procedure was as follow: pre-denature at 94 °C for 2 min, followed by 30 cycles of 94 °C for 15 s, 49 °C for 30 s, and 68 °C for 60 s, final extension at 68 °C for 5 min, and terminated at 4 °C. The PCR results were analyzed on a 3% agarose gel stained by SYBR Green I.

RESULTS

Principle and Design of Dual-Apt and CA-RCA. The principle and design of the established strategy was shown in Scheme 1. Two aptamers, one for binding and enriching the bacteria (A-Apt) and the other for generating a visualized signal (D-Apt), were used in this strategy. First of all, two aptamers binding to different transmembrane proteins were incubated with the pathogen cells.[25−27] Then, the SMBs were added to the mixture to capture the target bacteria via the biotin-modified A-Apt. The SMBs loading the A-Apt−bacteria−D-Apt complexes were separated and washed 3 times with buffer solution. Then, the enriched D-Apt was used as the template for CA-RCA.

In the CA-RCA step, D-Apt was amplified through the RCA mechanism to generate visible signals (sequences in Table 1). The D-Apt was designed with an aptamer sequence specifically binding to *V. parahaemolyticus* and a complementary G4 sequence that encodes a G4 structure via the RCA reaction. Besides, recognition sites of two nicking enzymes (Nb.BbvCI and Nb.BtsI) were also embedded into the D-Apt to release the G4 sequence from the RCA products. The D-Apt was first circularized by T4 DNA ligase and then amplified by Φ29 DNA polymerase via the linear RCA mechanism. The two nicking enzymes were introduced in the RCA system to cut the G4 sequence out of the RCA products that are long single strands consisting of tandemly repeated complementary D-Apt sequences. The G4 structure complexing with a hemin molecule served as an enzyme to catalyze the oxidation of $ABTS^{2-}$ to $ABTS^{\bullet -}$, generating a green color for the naked eye. Therefore, a lower concentration of *V. parahaemolyticus* in food samples can be visually detected by Dual-Apt and CA-RCA.

Fabrication of CA-RCA To Amplify D-Apt Generating a G4 Sequence. Traditionally, RCA using DNA polymerase with strand displacement activity was employed to amplify the circular amplicon. The amplification rate of linear RCA that produces a single-stranded product is only 10^3-fold, which is not able to generate detectable signals for bacteria with lower concentrations.[28] To fix the problem, a novel CA-RCA method was developed to enhance the amplification rate of linear RCA. The D-Apt was used as the template for validation. As shown in Figure 1A, amplification products from traditional RCA were observed at the top of the gel. With the introduction of a certain amount of Nb.BbvCI and Splint-BbvCI, the amount of RCA products was significantly increased. This can be ascribed to fact that Nb.BbvCI can cut the nascent strand out of the circular amplicon, a process that released the strain imposed by the nascent strand, which, in turn, helped the restoration of the polymerization speed of the Φ29 DNA polymerase, generating more RCA products.[29] The addition of Nb.BtsI and Splint-BtsI in the RCA reaction also changed the form of the products, however, into a series of cut fragments varying in length of 1 unit of D-Apt difference. When the two enzymes and their splints were added to the RCA reaction altogether, dramatically increased RCA products were obtained, with the digested single G4 sequence observed at the bottom of the gel. This indicated that the CA-RCA not only increased the amount of RCA products but also delivered the digested monomer G4 sequence, which paves the way for subsequent visualized detections. On the basis of the amount of final

DOI: 10.1021/acs.jafc.8b04913
J. Agric. Food Chem. 2019, 67, 1244−1253

products and initial template, it was calculated that CA-RCA with dual nicking enzymes can provide a ca. 10^6 amplification rate. Optimization of the concentrations of the two nicking enzymes can be found in Figure S1 of the Supporting Information.

The products from the four types of RCA reactions were used to catalyze the oxidation of $ABTS^{2-}$ to $ABTS^{\bullet -}$ to produce the visual signal. As shown in Figure 1B, products of the traditional RCA failed to catalyze the coloration reaction (no green color observed). This is probably because, although the G4 sequence in the long-strand RCA products can fold into a quadruplex structure, steric hindrance and transient base paring from the adjacent part of the strand seriously lower its catalytic efficiency.[30] The coloration reaction catalyzed by RCA with Nb.BbvCI barely delivered a green color, which was consistent with the electrophoretic result demonstrating that no monomeric G4 sequence was produced. For the same reaction catalyzed by RCA with Nb.Btsl, a light green color was observed. As expected, a distinct green color was developed by the product of the RCA reaction with the two enzymes, indicating that the G4 structure generated by CA-RCA successfully catalyzed the oxidation of $ABTS^{2-}$ to $ABTS^{\bullet -}$. Absorbance of the four reactions was shown in Figure 1C, manifesting that CA-RCA with two nicking enzymes delivered the strongest colorimetric signal from the same amount of D-Apt template. Therefore, the CA-RCA method to amplify the D-Apt generating a visualized signal for detection was established.

Detection of *V. parahaemolyticus* Using the Established Strategy. To validate the strategy for *V. parahaemolyticus* detection, experiments were carried out using a serial diluted bacteria suspension (from 10^6 to 10 CFU/mL). A-Apt was used to separate and enrich the bacterium, while the D-Apt binding on the surface of the enriched pathogen served as the probe to provide optical signals. An optimization experiment was performed to determine the concentration of the aptamers as 0.05 μM (data not shown). Lower concentrations of both aptamers will take more time for target cell recognition and binding, leading to a prolonged incubation. For A-Apt, a higher concentration would cause a waste and had no conducive effect on target cell binding. D-Apt with a concentration more than 1.0 μM might cause false-positive results, on account of the non-specific adsorption of the aptamer on the magnetic beads. The amplification results of D-Apt from *V. parahaemolyticus* varying in concentration were shown in Figure 2A. CA-RCA generated two types of products: one represented the complementary D-Apt sequence, and the other was G4. No band was observed from the tube void of the pathogen cells, indicating that the cross-paring of the two aptamers, which may cause false-positive results, was effectively avoided here. Therefore, the amplification products were exclusively designated to the presence of *V. parahaemolyticus*. On the other hand, even if the sample contained 10^6 CFU/mL of target bacterium, reactions missing any one of the two aptamers still failed to deliver any products, suggesting that the strategy was validated with specificity imparted by the two aptamers altogether. The existence of *V. parahaemolyticus* can be directly determined by the naked eye based on the green color of $ABTS^{\bullet -}$ generated by the CA-RCA products (Figure 2B). The absorption spectra of the samples containing different concentrations of *V. parahaemolyticus* were shown in Figure 2C, demonstrating that the intensity of the color was in direct proportion to the concentration of *V. parahaemolyticus*

Table 1. Sequence of Oligomers Used in CA-RCA[a]

name	sequence (5′ → 3′)	length (nt)
A-Apt	TACGACCAGAATCTAAAAATGGGCAAAGAAACAGTGACTCGTTGAGATACTTATGTGCGTCAAAAAAAAA-b	84
D-Apt	p-*CCTCAGC*ATAAGCATGAATTGACCAACCTAAACTTATTCATTTTCCAGCACCTCTAATATTACTGGC**GCAGTGCACCCACCCACCCACCC**	90
Splint-L	GCTGAGGGGGTGGG	14
Splint-BbvCI	CCCACCCCCTCAGC-p	14
Splint-Btsl	TGGCGCAGTGCAC-p	13

[a]The bold letters indicate the sequence that encodes a G4 structure in products. The italic sequences are used for circularization with the help of Splint-L. The underlined bases are recognition sites for Nb.BbvCI and Nb.Btsl, respectively. "b" represents a biotin modification, "p" indicates a 3′-end phosphorylation that prevents the elongation from the splint by Φ29 DNA polymerase.

DOI: 10.1021/acs.jafc.8b04913
J. Agric. Food Chem. 2019, 67, 1244−1253

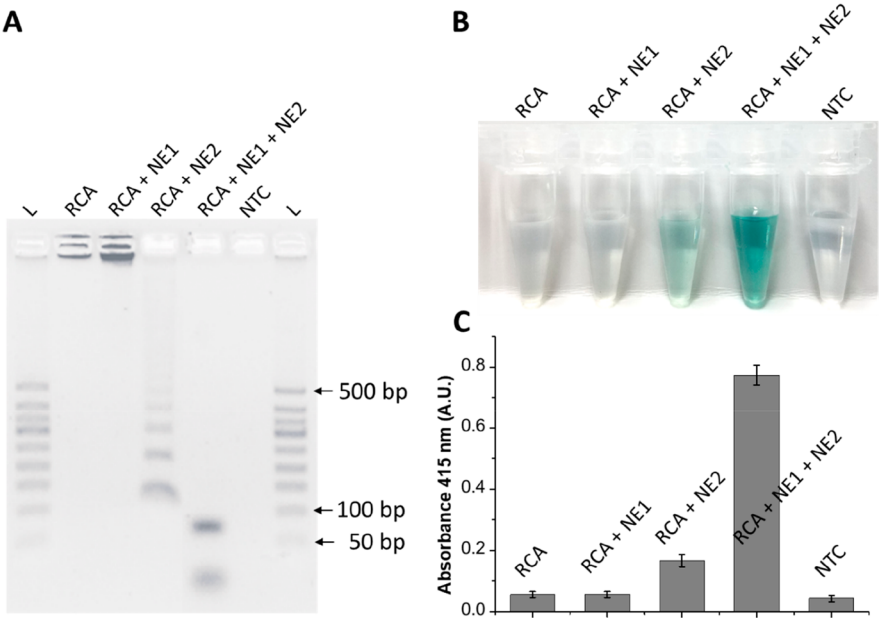

Figure 1. CA-RCA developed to amplify the D-Apt for visualized detection. (A) Products from four types of RCA to amplify the D-Apt. L represents a 50 bp ladder. Nb.BbvCI of 0.1 unit and Nb.BtsI of 5 units were added to the RCA reaction, with the corresponding splint of 1.0 μM. (B) Coloration reactions catalyzed by the products from the RCA reactions. (C) Absorbance of the corresponding solutions in panel B. NE1 represents Nb.BbvCI, and NE2 indicates Nb.BtsI.

cells. The calibration plot of the logarithm of the bacterium concentration against color intensity was fabricated as well. As seen in Figure 2D, a good linear correlation curve was obtained in the range from 10^6 to 10 CFU/mL, suggesting that the established strategy was capable of performing relative quantification analysis of *V. parahaemolyticus*.

The specificity study was carried out by detecting other common pathogens, including *E. coli*, *L. monocytogenes*, *S. typhimurium*, *S. dysenteriae*, and *S. aureus*, and the detailed operation process can be found in the Supporting Information. As seen in Figure 2E, only the presence of *V. parahaemolyticus* in the single or mixed condition rendered a dramatic increase of green color, while other bacteria triggered no visualized signals. The mean optical intensities of three parallel samples corresponding to results in the specificity study were shown in Figure 2F. The color signal of the target pathogen is significantly higher than that of the other reference bacteria, demonstrating again that the developed strategy is applicable for the selective detection of *V. parahaemolyticus*. The desirable specificity for the target pathogen can be ascribed to the two functional aptamers, which were obtained by an advanced cell SELEX protocol that we recently established (paper published elsewhere). During the screening process for the *V. parahaemolyticus*-specific aptamers, non-specific ssDNA was eliminated for the low affinity. Meanwhile, *E. coli*, *L. monocytogenes*, and *S. typhimurium* were used as the counter targets to incubate with the aptamer candidates that bind to *V. parahaemolyticus* cells, a process that effectively rules out the cross-binding of the selected aptamers to the other common foodborne pathogens. Besides, only *V. parahaemolyticus* cells, which can be simultaneously recognized by the two aptamers, would result in visible signals, a property that contributed to the high selectivity of Dual-Apt and CA-RCA.

Analysis of the Contamination of *V. parahaemolyticus* in Food Samples. The *V. parahaemolyticus*-susceptible foods, including oyster, clam, codfish, jellyfish, shrimp, milk, and squid, were used as the possible host. The food samples were commercially gained, confirmed to be *V. parahaemolyticus*-negative, and then spiked with *V. parahaemolyticus* cells varying in concentration. Proteinase K was applied in some cases, because the presence of large protein molecules could inhibit the ligation and amplification reactions, resulting in false-negative results.[31] As shown in Figure 3A, all of the bacteria-positive food samples were observed with a green color and the optical intensity was basically in direct proportion to the concentration of pathogen cells. When the amount of *V. parahaemolyticus* cells dropped down to less than 10 CFU/mL (g), no green color can be observed or detected by a spectrophotometer. Therefore, the limit of detection (LOD) of the established strategy was determined as 10 CFU/mL (g), which is comparable to that of the advance biosensors reported recently.[19,32] Food samples free from the pathogen contamination can be clearly determined, because the absorbance of no bacteria control samples [*V. parahaemolyticus* of 0 CFU/mL (g)] at 415 nm was as low as the blank control used in colorimetric operation (Figure 3B). The detection results provided by Dual-Apt and CA-RCA were also confirmed using hyper-branched RCA, amplifying the D-Apt with two specific primers and SYBR Green staining (Figure S2 of the Supporting Information). These results combined indicated that the biosensor developed in this study was capable of detecting the target bacteria in food samples and can be applied as a promising method in food monitoring and government.

Comparison to Conventional Culture-Based Counting and PCR Methods for *V. parahaemolyticus* Detection. The *V. parahaemolyticus*-contaminated oyster was used as the sample for the comparison study. Parallel prepared oyster samples with pathogen concentrations from 10^4 to 0 CFU/mL were subjected to the detection using the three methods. As seen in Figure 4A, numbers of colonies were formed on the bacteria-positive samples, which were consistent

DOI: 10.1021/acs.jafc.8b04913
J. Agric. Food Chem. 2019, 67, 1244−1253

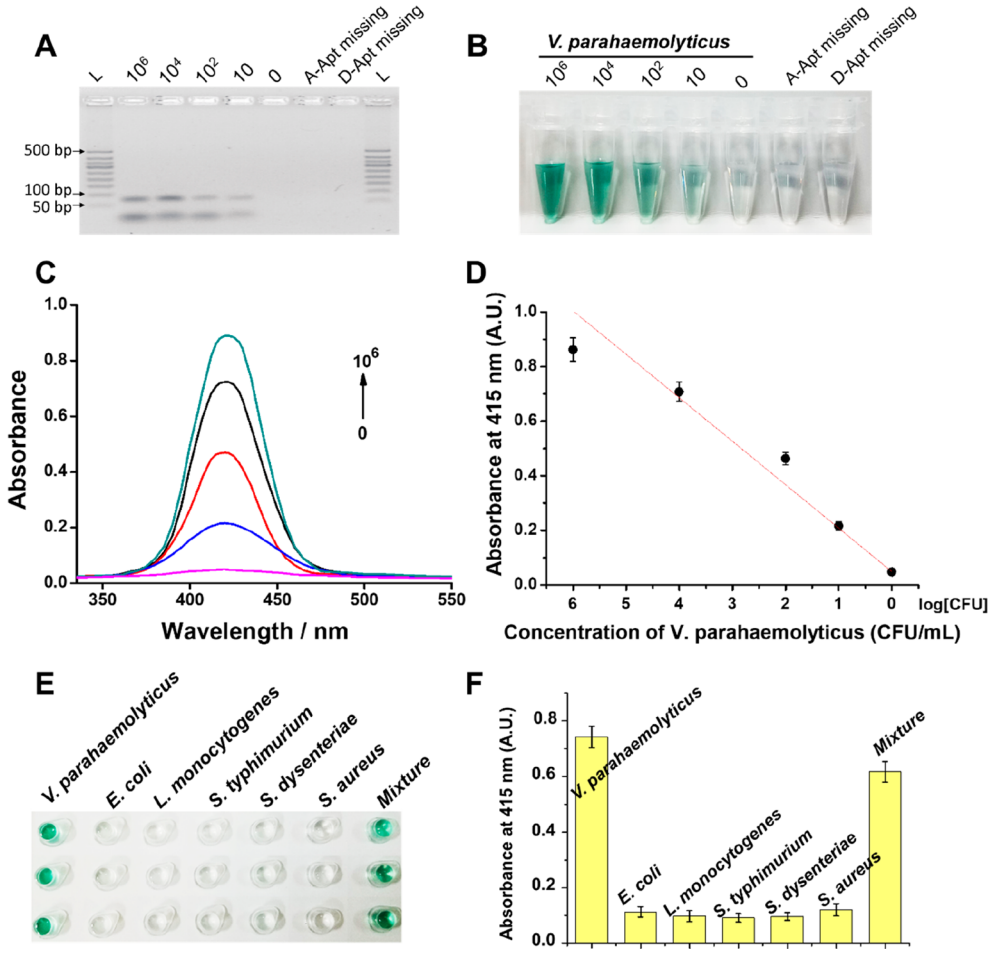

Figure 2. Detection of *V. parahaemolyticus* using Dual-Apt and CA-RCA. (A) Sensitivity of the established strategy. L represented a 50 bp ladder. For reactions missing A-Apt or D-Apt, 10^6 CFU/mL of *V. parahaemolyticus* was applied. (B) Visualized detection of *V. parahaemolyticus* varying in concentration. (C) Absorption spectra of the visualized detection results presented in panel B. (D) Linear correlation curve for detecting various concentrations of *V. parahaemolyticus*. The error bars represented the standard deviation of three parallel experiments. (E) Specificity of Dual-Apt and CA-RCA to detect *V. parahaemolyticus* among several common foodborne pathogens. Each bacterium was tested in triplicate, and the concentration of the pathogens was 10^6 CFU/mL. For the mixed bacteria (mixture), 10^5 CFU/mL of each pathogen was applied. (F) Absorbance of the results from the specificity study. The mean value of the three parallel reactions was recorded, and the standard deviations were reflected by the error bars.

with the initial concentration of the pathogen in oysters. The PCR also detected the presence of the bacterium, demonstrating a detection limit of 10 CFU/mL (Figure 4B). For Dual-Apt and CA-RCA, bacteria-positive samples were detected with visualized signals. The level of *V. parahaemolyticus* infection can be directly obtained on the basis of the intensity of the green color (Figure 4C). On the basis of consistent results, the culture-based and PCR methods confirmed the established strategy with high sensitivity and specificity. The whole process of Dual-Apt and CA-RCA can be consummated within 2 h, which is another advantage because the operation of culture-based counting requires at least 48 h.[23] Although the PCR-based methods can provide results in hours, the interpretation has to rely on gel-imaging or fluorescence instruments.[33] In comparison to that, results from Dual-Apt and CA-RCA can be immediately read out by the naked eye, making it more applicable for on-spot detection. To demonstrate the applicability of the established method, 10 *V. parahaemolyticus*-suspected oyster samples provided by a local inspection and quarantine center were subjected to the visualized detection. These real samples were also analyzed by the conventional culture-based method to validate the results of the visualized detection (a detailed procedure can be found in the Supporting Information). As shown in Figure 4D, the presence of *V. parahaemolyticus* in the real samples can be detected by Dual-Apt and CA-RCA. No color was observed after the visualized detection for S3, S4, and S7; therefore, those samples could be determined as *V. parahaemolyticus*-negative (confirmed by the culture-based method). A relatively intensive green color was observed for S1, S5, and S10, indicating that those oyster samples were seriously infected with *V. parahaemolyticus* and should be banned from the market. The color intensity was in direct proportion to the counts of CFU on the plate, suggesting that the established method can be used for relative quantitation of *V. parahaemolyticus* contamination in real food samples.

DISCUSSION

Rapid and accurate detection of pathogens in real food samples is a worldwide challenge. Apart from the traditional culture-based counting method, the advanced technologies proposed can be divided into two categories: antibody- and nucleic-acid-

DOI: 10.1021/acs.jafc.8b04913
J. Agric. Food Chem. 2019, 67, 1244−1253

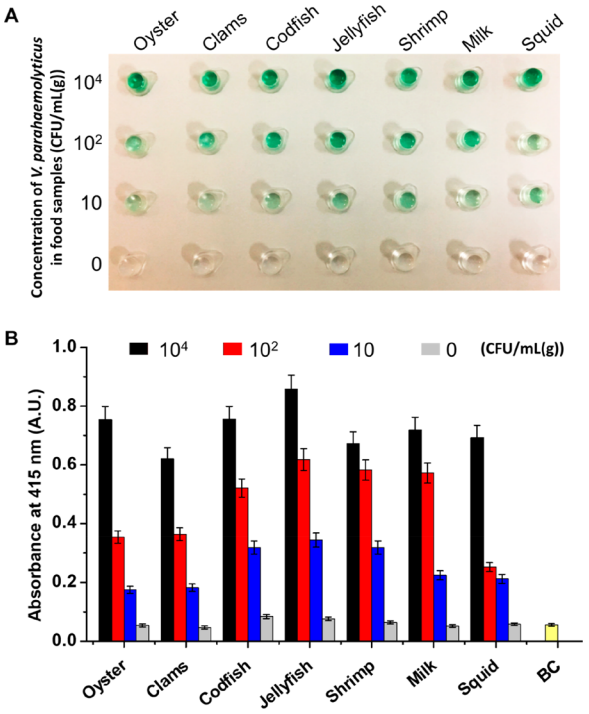

Figure 3. Detection of *V. parahaemolyticus* in food samples. (A) Typical results of the visualized detection of foods contaminated by the bacterium varying in concentration. The confirmed *V. parahaemolyticus*-negative food samples spiked with an indicated number of the pathogen cells were subjected to detection. (B) Histogram of absorbance at 415 nm of samples corresponding to that in panel A. The mean value of the three parallel samples was recorded, and the standard deviations were reflected by the error bars. "BC" represented the blank control used in colorimetric operation.

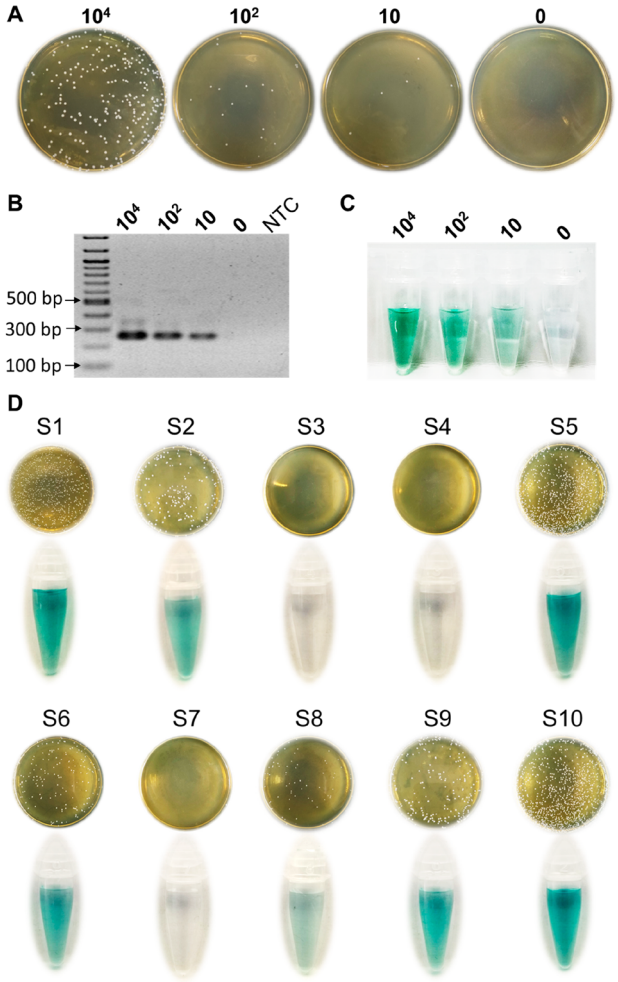

Figure 4. Comparison of the established strategy to plate counting and PCR. (A) Detection of *V. parahaemolyticus* in oyster using culture plate counting. From left to right, the plates were coated with oyster homogenate spiked with *V. parahaemolyticus* from 10^4 to 0 CFU/mL. (B) PCR detection of *V. parahaemolyticus* in oyster samples. (C) Detection of *V. parahaemolyticus* in oyster samples by Dual-Apt and CA-RCA. (D) Analyzing the contamination levels of *V. parahaemolyticus* in real food samples by Dual-Apt and CA-RCA and culture-based methods.

based strategies.[34] In this study, we developed a visualized detection strategy (Dual-Apt and CA-RCA) using an aptamer, a single-stranded nucleic acid sequence with affinity and specificity comparable to that of the antibody. The aptamers used in this study were selected from a random ssDNA library by a novel cell SELEX method (paper published elsewhere) using *V. parahaemolyticus* as the target. Only aptamer candidates of high affinities to the target cells can survive the stringent selection process, which guarantees the high specificity of the aptamers. Aptamers obtained from cell SELEX were proven to be able to bind the transmembrane proteins on the surface of human and animal cells.[35] Besides, Hamula et al. proposed that the *Lactobacillus acidophilus*-specific aptamer was targeting S-layer protein on the cell surface.[26] Therefore, it stands a good chance that the membrane-embedded protein serves as the binding site for the specific aptamer.

One of the greatest strengths of an aptamer over an antibody is that it can amplify itself, generating exponentially augmented signals for detection.[36] RCA is a frequently used approach for detection. However, the traditional RCA can only provide less than 10^3 rate of amplification, which is not adequate for detection as a result of the possible cause of false-negative results.[37] Therefore, a novel RCA model, CA-RCA, was fabricated. Two nicking enzymes were introduced to the RCA step to digest the nascent long single strand that imposed resistance on the processing of Φ29 DNA polymerase. Once the long strand is removed from the circular amplicon, the rate of DNA synthesis by Φ29 DNA polymerase will increase to the initial level, generating more product than traditional RCA from the same amount of templates. Therefore, sensitivity of the CA-RCA-based detection is significantly enhanced.

The catalytic structure formed by the G4 sequence was employed here to deliver a visualized signal. Although it has been reported by several independent groups, we found that the G4 sequence in the long-strand RCA product barely produced any visible color.[38] Thus, two nicking enzymes was applied to cut the G4 sequence out of the long product, a process that significantly promoted the formation of G4 in the catalytic structure by eliminating the interference of the adjacent sequence.[39] The products of CA-RCA were two digested parts of complementary D-Apt sequence, a property that can effectively prevent the cross-contamination because the product is different from the initial template (D-Apt).

One of the biggest challenges to detect bacteria in a food sample is that the food composition, such as polysaccharides, protein, and lipid, could seriously inhibit the subsequent analysis reactions.[40] The more complex the food, the more

DOI: 10.1021/acs.jafc.8b04913
J. Agric. Food Chem. 2019, 67, 1244−1253

Table 2. Comparison to Recently Reported *V. parahaemolyticus* Detection Methods[a]

number	method used	linear range	LOD	reference
1	real-time PCR	10^2–10^6 CFU/g	112 CFU/g	43
2	SERS aptasensor	10–10^6 CFU/mL	10 CFU/mL	44
3	SERS aptasensor	1–10^8 CFU/mL	1 CFU/mL	42
4	AuNPs–HRP aptasensor	10–10^6 CFU/mL	10 CFU/mL	22
5	AuNPs–Mn^{2+} immunoassay	10–10^6 CFU/mL	10 CFU/mL	10
6	microfluidic chip	10^3–10^6 CFU/mL	10^3 CFU/mL	45
7	visualized CA-RCA aptasensor	10–10^6 CFU/mL	10 CFU/mL	current study

[a]SERS represents surface-enhanced Raman scattering, and AuNPs and HRP indicate gold nanoparticles and horseradish peroxidase, respectively.

uncertain the detection results could be. With that taken into consideration, we introduced SMBs that effectively remove the background composition into the established strategy. Besides, SMBs can enrich the target bacteria from the sample solution in virtue of the A-Apt, contributing to the enhanced detection sensitivity. The results of detecting *V. parahaemolyticus* in the real food samples demonstrated that the introduction of SMBs can effectively eliminate the interference imposed by the food matrix, a property that will enable the established method applicability for monitoring foodborne pathogens in the application area. High-throughput analysis is also an irreconcilable requirement for detecting pathogen-suspected food samples. As a result of the isothermal nature of CA-RCA that can be performed under a constant temperature, the Dual-Apt and CA-RCA strategy can simultaneously analyze a large number of samples on an enzyme-linked immunosorbent assay (ELISA) plate. Therefore, a high-throughput, on-spot detecting device is promising to be created on the basis of the strategy that we developed in this study.

Plate counting and PCR are classic methods to detect foodborne pathogens and also serve as the basis for national food inspection standards. Although the two methods are reliable and robust with good specificity and reproducibility, the time-consuming operation process and requirement of specialized equipment and highly trained personnel denied their application for rapid on-spot detection.[41] Duan et al. and Yao et al. reported several aptamer-based strategies for *V. parahaemolyticus* detection.[19−21,42] Those methods were demonstrated to be feasible; however, they still need analytical instruments, such as flow cytometry, Raman spectrometer, or ultraviolet (UV) lamp, to interpret the results. A comparison of Dual-Apt and CA-RCA with newly reported methods on *V. parahaemolyticus* detection was summarized in Table 2. It can be inferred that the current strategy is of comparable performance to most of the new methods in terms of linear range and LOD, although the sensitivity and dynamic range are lower than those of a Raman spectrograph-based aptasensor fabricated by Yao et al.[42]

In this study, rapid and visualized detection of *V. parahaemolyticus* is realized by Dual-Apt and CA-RCA, which directly provides visible results for the naked eye. Several advantages combined makes our strategy a promising point of care biosensor for on-spot detection. First, the time-consuming DNA extraction that is necessary for PCR-based methods can be avoided here as a result of the two aptamers that specifically bind to transmembrane proteins of the target bacterium. Second, strong amplification potential of CA-RCA developed in this study allowed for the detection of a pathogen with a lower concentration in food. Third, the well-designed D-Apt not only recognizes the target pathogen but also encodes G4 structures, enabling visualized interpretation of the results. The advanced studies on the detection of other foodborne pathogens and how to integrate the sample treatment and detection processes into a portable device for on-spot application are in progress.

In conclusion, we developed here an aptamer-based strategy for visualized detection of *V. parahaemolyticus* powered by CA-RCA. Dual bacteria-specific aptamers, one for collecting and enriching pathogen cells and the other for visual signal detection, were employed. CA-RCA with two nicking enzymes in the amplification system was fabricated to amplify the D-Apt, which encodes a G4 structure catalyzing $ABTS^{2-}$ to generate colorful signals. High detection sensitivity was achieved by SMB magnetic separation that effectively removes the inhibitory factors from food composition as well as enriches the target bacterium for CA-RCA detection. *V. parahaemolyticus* in several foods was successfully detected with LOD as low as 10 CFU/mL (g). The established strategy is proven to be of sensitivity and specificity comparable to that of the classic methods, with the advantages being free from DNA extraction, visualized signal output, and no requirement of a precision thermal cycler. Detection of other foodborne pathogens in commercial goods is promising to be realized using different bacteria-specific aptamers, demonstrating that the strategy is of enormous application potential in the food safety control area.

■ ASSOCIATED CONTENT

Supporting Information

The Supporting Information is available free of charge on the ACS Publications website at DOI: 10.1021/acs.jafc.8b04913.

Optimization of two nicking enzymes for CA-RCA fabrication, confirmation of the detection results of Dual-Apt and CA-RCA by hyper-branched RCA, specificity investigation of Dual-Apt and CA-RCA for *V. parahaemolyticus* detection, and visualized detection of *V. parahaemolyticus* in real food samples (PDF)

■ AUTHOR INFORMATION

Corresponding Authors

*Telephone/Fax: +86-29-85310580. E-mail: wangxingyu@snnu.edu.cn.

*Telephone/Fax: +86-29-85310580. E-mail: xbyang@snnu.edu.cn.

ORCID

Xingyu Wang: 0000-0003-4000-464X

Xingbin Yang: 0000-0002-8039-0525

Funding

This work was supported by the National Natural Science Foundation of China (C31671823), the National Natural Science Foundation for Young Scholars of China (81601877),

DOI: 10.1021/acs.jafc.8b04913
J. Agric. Food Chem. 2019, 67, 1244−1253

the Key R&D Program of Shaanxi Province (2018NY-095), and the Fundamental Research Funds for the Central Universities (GK201603101).

Notes

The authors declare no competing financial interest.

REFERENCES

(1) Liu, J. M.; Wang, Z. H.; Ma, H.; Wang, S. Probing and quantifying the food-borne pathogens and toxins: From *in vitro* to *in vivo*. *J. Agric. Food Chem.* **2018**, *66*, 1061−1066.

(2) Shin, J. H.; Hong, J.; Go, H.; Park, J.; Kong, M.; Ryu, S.; Kim, K. P.; Roh, E.; Park, J. K. Multiplexed detection of foodborne pathogens from contaminated lettuces using a handheld multistep lateral flow assay device. *J. Agric. Food Chem.* **2018**, *66*, 290−297.

(3) Yeung, P. S.; Boor, K. J. Epidemiology, pathogenesis, and prevention of foodborne *Vibrio parahaemolyticus* infections. *Foodborne Pathog. Dis.* **2004**, *1*, 74−88.

(4) Wang, Y.; Liu, S. J.; Pu, Q. K.; Li, Y. X.; Wang, X. X.; Jiang, Y.; Yang, D. N.; Yang, Y.; Yang, J. L.; Sun, C. J. Rapid identification of *Staphylococcus aureus*, *Vibrio parahaemolyticus* and *Shigella sonnei* in foods by solid phase microextraction coupled with gas chromatography-mass spectrometry. *Food Chem.* **2018**, *262*, 7−13.

(5) De Paola, A.; Nordstrom, J. L.; Bowers, J. C.; Wells, J. G.; Cook, D. W. Seasonal abundance of total and pathogenic *Vibrio parahaemolyticus* in Alabama oysters. *Appl. Environ. Microbiol.* **2003**, *69*, 1521−1526.

(6) Lozano-León, A.; Torres, J.; Osorio, C. R.; Martínez-Urtaza, J. Identification of TDH-positive *Vibrio parahaemolyticus* from an outbreak associated with raw oyster consumption in Spain. *FEMS Microbiol. Lett.* **2003**, *226*, 281−284.

(7) Zhong, Q.; Tian, J.; Wang, B.; Wang, L. PMA based real-time fluorescent LAMP for detection of *Vibrio parahaemolyticus* in viable but nonculturable state. *Food Control* **2016**, *63*, 230−238.

(8) Wu, W.; Zhou, M.; He, H.; Liu, C. Z.; Li, P. F.; Wang, M.; Liu, Y.; Hao, X. D.; Fang, Z. Y. A sensitive aptasensor for the detection of *Vibrio parahaemolyticus*. *Sens. Actuators, B* **2018**, *272*, 550−558.

(9) Arora, K.; Chand, S.; Malhotra, B. D. Recent developments in bio-molecular electronics techniques for food pathogens. *Anal. Chim. Acta* **2006**, *568*, 259−274.

(10) Fu, K. Y.; Zheng, Y.; Li, J.; Liu, Y. S.; Pang, B.; Song, X. L.; Xu, K.; Wang, J.; Zhao, C. Colorimetric immunoassay for rapid detection of *Vibrio parahaemolyticus* based on Mn^{2+} mediates the assembly of gold nanoparticles. *J. Agric. Food Chem.* **2018**, *66*, 9516−9521.

(11) Kim, J.; Demeke, T.; Clear, R. M.; Patrick, S. K. Simultaneous detection by PCR of *Escherichia coli Listeria monocytogenes* and *Salmonella typhimurium* in artificially inoculated wheat grain. *Int. J. Food Microbiol.* **2006**, *111*, 21−25.

(12) Tuerk, C.; Gold, L. Systematic evolution of ligands by exponential enrichment: RNA ligands to bacteriophage T4 DNA polymerase. *Science* **1990**, *249*, 505−510.

(13) Bunka, D.; Stockley, P. Aptamers come of age-at last. *Nat. Rev. Microbiol.* **2006**, *4*, 588−596.

(14) Aquino-Jarquin, G.; Toscano-Garibay, J. D. RNA aptamer evolution: Two decades of selection. *Int. J. Mol. Sci.* **2011**, *12*, 9155−9171.

(15) Song, S.; Wang, L.; Li, J.; Fan, C.; Zhao, J. Aptamer-based biosensors. *TrAC, Trends Anal. Chem.* **2008**, *27*, 108−117.

(16) Cao, X.; Li, S.; Chen, L.; Ding, H.; Xu, H.; Huang, Y.; Li, J.; Liu, N.; Cao, W.; Zhu, Y.; Shen, B.; Shao, N. Combining use of a panel of ssDNA aptamers in the detection of *Staphylococcus aureus*. *Nucleic Acids Res.* **2009**, *37*, 4621−4628.

(17) Fischer, C.; Hünniger, T.; Jarck, J. H.; Frohnmeyer, E.; Kallinich, C.; Haase, I.; Hahn, U.; Fischer, M. Food sensing: Aptamer-based trapping of *Bacillus cereus* spores with specific detection via real time PCR in milk. *J. Agric. Food Chem.* **2015**, *63*, 8050−8057.

(18) Zhao, Q.; Lu, X.; Yuan, C. G.; Li, X. F.; Le, X. C. Aptamer-linked assay for thrombin using gold nanoparticle amplification and inductively coupled plasmamass spectrometry detection. *Anal. Chem.* **2009**, *81*, 7484−7489.

(19) Duan, N.; Wu, S. J.; Yu, Y.; Ma, X. Y.; Xia, Y.; Chen, X. J.; Huang, Y. K.; Wang, Z. P. A dual-color flow cytometry protocol for the simultaneous detection of *Vibrio parahaemolyticus* and *Salmonella typhimurium* using aptamer conjugated quantum dots as labels. *Anal. Chim. Acta* **2013**, *804*, 151−158.

(20) Duan, N.; Wu, S. J.; Dai, S.; Miao, T. T.; Chen, J.; Wang, Z. P. Simultaneous detection of pathogenic bacteria using an aptamer based biosensor and dual fluorescence resonance energy transfer from quantum dots to carbon nanoparticles. *Microchim. Acta* **2015**, *182*, 917−923.

(21) Duan, N.; Shen, M. F.; Wu, S. J.; Zhao, C. X.; Ma, X. Y.; Wang, Z. P. Graphene oxide wrapped Fe_3O_4@Au nanostructures as substrates for aptamer-based detection of *Vibrio parahaemolyticus* by surface-enhanced Raman spectroscopy. *Microchim. Acta* **2017**, *184*, 2653−2660.

(22) Wu, S.; Wang, Y.; Duan, N.; Ma, H.; Wang, Z. Colorimetric aptasensor based on enzyme for the detection of *Vibrio parahaemolyticus*. *J. Agric. Food Chem.* **2015**, *63*, 7849−7854.

(23) Hara-Kudo, Y.; Nishina, T.; Nakagawa, H.; Konuma, H.; Hasegawa, J.; Kumagai, S. Improved method for detection of *Vibrio parahaemolyticus* in seafood. *Appl. Environ. Microb.* **2001**, *67*, 5819−5823.

(24) Zarei, M.; Borujeni, M. P.; Jamnejad, A.; Khezrzadeh, M. Seasonal prevalence of *Vibrio* species in retail shrimps with an emphasis on *Vibrio parahaemolyticus*. *Food Control* **2012**, *25*, 107−109.

(25) Mallikaratchy, P.; Tang, Z.; Kwame, S.; Meng, L.; Shangguan, D.; Tan, W. Aptamer directly evolved from live cells recognizes membrane bound immunoglobin heavy mu chain in Burkitt's lymphoma cells. *Mol. Cell. Proteomics* **2007**, *6*, 2230−2238.

(26) Hamula, C. L.; Zhang, H.; Guan, L. L.; Li, X. F.; Le, X. C. Selection of aptamers against live bacterial cells. *Anal. Chem.* **2008**, *80*, 7812−7819.

(27) Meyer, M.; Scheper, T.; Walter, J. G. Aptamers: Versatile probes for flow cytometry. *Appl. Microbiol. Biotechnol.* **2013**, *97*, 7097−7109.

(28) Lizardi, P. M.; Huang, X.; Zhu, Z.; Bray-Ward, P.; Thomas, D. C.; Ward, D. C. Mutation detection and single-molecule counting using isothermal rolling-circle amplification. *Nat. Genet.* **1998**, *19*, 225−232.

(29) Kuhn, H.; Demidov, V. V.; Frank-Kamenetskii, M. D. Rolling-circle amplification under topological constraints. *Nucleic Acids Res.* **2002**, *30*, 574−580.

(30) Dahl, F.; Banér, J.; Gullberg, M.; Mendel-Hartvig, M.; Landegren, U.; Nilsson, M. Circle-to-circle amplification for precise and sensitive DNA analysis. *Proc. Natl. Acad. Sci. U. S. A.* **2004**, *101*, 4548−4553.

(31) Nelson, J. R.; Cai, Y. C.; Giesler, T. L.; Farchaus, J. W.; Sundaram, S. T.; Ortiz-Rivera, M.; Hosta, L. P.; Hewitt, P. L.; Mamone, J. A.; Palaniappan, C.; Fuller, C. W. TempliPhi, Φ29 DNA polymerase based rolling circle amplification of templates for DNA sequencing. *BioTechniques* **2002**, *32*, S44−S47.

(32) Wang, X. Y.; Yu, X.; Wang, X. L.; Suzuki, M.; Asanuma, H.; Dong, P.; Wu, W.; Liang, X. G. Highly specific DNA detection from massive background nucleic acids based on rolling circle amplification of target dsDNA. *RSC Adv.* **2014**, *4*, 38293−38299.

(33) Kosman, J.; Juskowiak, B. Peroxidase-mimicking DNAzymes for biosensing applications: A review. *Anal. Chim. Acta* **2011**, *707*, 7−17.

(34) Velusamy, V.; Arshak, K.; Korostynska, O.; Oliwa, K.; Adley, C. An overview of foodborne pathogen detection: In the perspective of biosensors. *Biotechnol. Adv.* **2010**, *28*, 232−254.

(35) Hicke, B. J.; Stephens, A. W.; Gould, T.; Chang, Y. F.; Lynott, C. K.; Heil, J.; Borkowski, S.; Hilger, C. S.; Cook, G.; Warren, S.; Schmidt, P. G. Tumor targeting by an aptamer. *J. Nucl. Med.* **2006**, *47*, 668−678.

DOI: 10.1021/acs.jafc.8b04913
J. Agric. Food Chem. 2019, 67, 1244−1253

(36) Fang, X.; Tan, W. H. Aptamers generated from cell-SELEX for molecular medicine: A chemical biology approach. *Acc. Chem. Res.* **2010**, *43*, 48−57.
(37) Liu, D.; Daubendiek, S. L.; Zillman, M. A.; Ryan, K.; Kool, E. T. Rolling circle DNA synthesis: Small circular oligonucleotides as efficient templates for DNA polymerases. *J. Am. Chem. Soc.* **1996**, *118*, 1587−1594.
(38) Tian, Y.; He, Y.; Mao, C. D. Cascade signal amplification for DNA detection. *ChemBioChem* **2006**, *7*, 1862−1864.
(39) Deng, M.; Zhang, D.; Zhou, Y.; Zhou, X. Highly effective colorimetric and visual detection of nucleic acids using an asymmetrically split peroxidase DNAzyme. *J. Am. Chem. Soc.* **2008**, *130*, 13095−13102.
(40) Law, J. W.-F.; Ab Mutalib, N.-S.; Chan, K.-G.; Lee, L.-H. Rapid methods for the detection of foodborne bacterial pathogens: Principles, applications, advantages and limitations. *Front. Microbiol.* **2015**, *5*, 770−788.
(41) Lin, Y. H.; Chen, S. H.; Chuang, Y. C.; Lu, Y. C.; Shen, T. Y.; Chang, C. A.; Lin, C. S. Disposable amperometric immunosensing strips fabricated by Au nanoparticles-modified screen-printed carbon electrodes for the detection of foodborne pathogen *Escherichia coli* O157:H7. *Biosens. Bioelectron.* **2008**, *23*, 1832−1837.
(42) Yao, L.; Ye, Y.; Teng, J.; Xue, F.; Pan, D.; Li, B.; Chen, W. *In vitro* isothermal nucleic acid amplification assisted surface-enhanced Raman spectroscopic (SERS) for ultrasensitive detection of *Vibrio parahaemolyticus*. *Anal. Chem.* **2017**, *89*, 9775−9780.
(43) Zhang, Z. H.; Xiao, L. L.; Lou, Y.; Jin, M. T.; Liao, C.; Malakar, P. K.; Pan, Y. J.; Zhao, Y. Development of a multiplex real-time PCR method for simultaneous detection of *Vibrio parahaemolyticus Listeria monocytogenes* and *Salmonella* spp. in raw shrimp. *Food Control* **2015**, *51*, 31−36.
(44) Duan, N.; Yan, Y. L.; Wu, S. J.; Wang, Z. P. *Vibrio parahaemolyticus* detection aptasensor using surface-enhanced Raman scattering. *Food Control* **2016**, *63*, 122−127.
(45) Pang, B.; Ding, X.; Wang, G. P.; Zhao, C.; Xu, Y. A.; Fu, K. Y.; Sun, J. J.; Song, X. L.; Wu, W. S.; Liu, Y. S.; Song, Q.; Hu, J. M.; Li, J.; Mu, Y. Rapid and quantitative detection of *Vibrio parahaemolyticus* by the mixed-dye-based loop-mediated isothermal amplification assay on a self-priming compartmentalization microfluidic chip. *J. Agric. Food Chem.* **2017**, *65*, 11312−11319.

DOI: 10.1021/acs.jafc.8b04913
J. Agric. Food Chem. 2019, 67, 1244−1253